

## HL-3 RESEARCH TOWARDS HIGH-PERFORMANCE PLASMA AND POWER EXHAUST SOLUTION

<sup>1</sup>W.L. Zhong, <sup>1</sup>X.Q. Ji, <sup>1</sup>W. Chen, <sup>1</sup>X.Y. Bai, <sup>2</sup>A. Bécoulet, <sup>3</sup>J. Bucalossi, <sup>1</sup>Z. Chen, <sup>4</sup>Z.P. Chen, <sup>1</sup>Y.H. Chen, <sup>5</sup>N. Conway, <sup>3</sup>L. Delpech, <sup>6</sup>P. Diamond, <sup>3</sup>A. Ekedahl, <sup>3</sup>J. Garcia, <sup>2</sup>Y. Gribov, <sup>4</sup>W.X. Guo, <sup>7</sup>Z.B. Guo, <sup>1</sup>G.Z. Hao, <sup>5</sup>J. Harrison, <sup>1</sup>M. Huang, <sup>3</sup>P. Huynh, <sup>8</sup>M. Isobe, <sup>9</sup>K. Imadera, <sup>1</sup>M. Jiang, <sup>2</sup>Y. Kamada, <sup>2</sup>S. Kim, <sup>5</sup>D. King, <sup>9</sup>Y. Kishimoto, <sup>1</sup>X.L. Liu, <sup>1</sup>B. Li, <sup>1</sup>J.X. Li, <sup>2</sup>A. Loarte, <sup>5</sup>F. Militello, <sup>8</sup>S. Morita, <sup>9</sup>K. Nagasaki, <sup>1</sup>L. Nie, K. <sup>1</sup>Ogawa<sup>8</sup>, <sup>2</sup>M. Schneider, <sup>1</sup>Z.B. Shi, <sup>5</sup>F. Rimini, <sup>5</sup>H.J. Sun, <sup>1</sup>R.H. Tong, <sup>1</sup>Y.Q. Wang, <sup>10</sup>X.G. Wang, <sup>1</sup>H.L. Wei, <sup>1</sup>G.L. Xiao, <sup>1</sup>L. Xue, <sup>4</sup>X. Xu, <sup>1</sup>Z.Y. Yang, <sup>1</sup>P.X. Yu, <sup>11</sup>Y. Yu, <sup>1</sup>B.D. Yuan, <sup>1</sup>F. Zhang, <sup>1</sup>J.Z. Zhang, <sup>1</sup>Y. Zhang, <sup>1</sup>Y.P. Zhang, <sup>1</sup>X. Zheng, <sup>3</sup>X.L. Zou, <sup>1</sup>M. Xu, <sup>1</sup>X.R. Duan, <sup>1</sup>Y. Liu, <sup>1</sup>L.B. Zhang, <sup>1</sup>Ye Liu and HL-3 team

<sup>1</sup>Southwestern Institute of Physics, PO Box 432, Chengdu 610041, China

<sup>2</sup>ITER Organization, 13067 Saint Paul Lez Durance Cedex, France

<sup>3</sup>CEA, IRFM, F-13108 Saint Paul Lez Durance, France

<sup>4</sup>Huazhong University of Science and Technology, Wuhan, China

<sup>5</sup>UKAEA, Culham Campus, Abingdon, Oxfordshire OX14 3DB, UK

<sup>6</sup>University of California San Diego, La Jolla, California 92093, United States of America

<sup>7</sup>Peking University, Beijing, China

<sup>8</sup>National Institute for Fusion Science, Oroshi, Toki, Gifu 509-5292, Japan

<sup>9</sup>Kyoto University, Uji, Kyoto, 611-0011, Japan

<sup>10</sup>Harbin Institute of Technology, Harbin 150006, China

<sup>11</sup>Sun Yat-sen University, Zhuhai 519082, China

Email: [zhongwl@swip.ac.cn](mailto:zhongwl@swip.ac.cn)

HL-3 is a large tokamak that is designed to operate at plasma current  $I_p = 3$  MA, toroidal field  $B_t = 3$  T, major radius  $R = 1.78$  m, minor radius  $a = 0.65$  m, elongation  $\kappa \leq 1.8$ , triangularity  $\delta > 0.5$ <sup>[1]</sup>. HL-3 has recently focused on high-current, high  $\beta_N$  discharges to achieve high performance plasma, establishing critical foundations for burning plasma research.

Since 2023, HL-3 has been undergoing major upgrades and is now a satellite facility of ITER, aiming at physics research and supporting future ITER operations<sup>[2]</sup>. To enable advanced high-performance plasma operation, major technical improvements include the installation of a 7 MW NBI at 120 kV, which increased the total auxiliary heating power to 18 MW. The implementation of a newly developed  $\pm 1$  kV/ $\pm 4$  kA vertical displacement event (VDE) fast control system has achieved a stable plasma elongation ratio of 1.7. Pioneering studies of plasma-wall interaction were undertaken with a hot-wall operation with the temperature above 100°C, laying the basis for fuel retention control which is an important topic for burning plasma like ITER. The plasma shape and position control precisions have been enhanced through the implementation of a GPU-accelerated real-time equilibrium reconstruction system, within  $\sim 0.6$  ms for a single time slice. The AI-enhanced CODIS system has shown good performance on controlling of the divertor configuration during extended discharges. The current diagnostics amount to over 40 specialized systems, such as the upgraded Thomson scattering system with expanded radial channels from 30 to 60 for improved resolution of the electron temperature/density profiles. A recently installed proton detection system successfully recorded fusion-generated protons. Other recently deployed diagnostics including fast-ion loss probes, an imaging neutral particle analyzer, and multiple neutron flux/energy spectrum measurement systems are also prepared for characterizing high performance fusion plasma operation.

Recent HL-3 research has prioritized advancing high-performance plasma scenarios, where significant progress has been demonstrated. HL-3 has enhanced its capability in routine operation at mega-ampere (MA) level plasma currents, and a maximum current of 1.6 MA has been obtained, with typical parameters as  $a = 0.63$  m,  $\kappa = 1.69$ ,  $\delta = 0.39$  and  $q_{95} \sim 3.0$ . Besides, H-mode operation with  $\sim 1.5$  MA plasma current has also been realized in lower single-null geometry. Systematic parametric investigations have been performed within H-mode scenarios, looking towards high performance and small/no ELM regimes. A novel "staircase" H-mode regime featuring a staircase-like ion temperature profile has been demonstrated, effectively mitigating edge layer collapse while preserving high

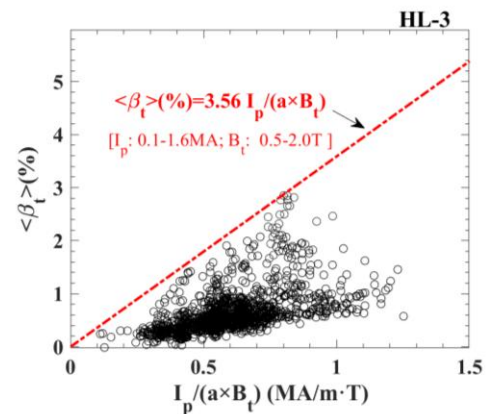


Fig.1 Statistical results of the relationship between the beta value and  $I_p/aB_t$  of HL-3 plasmas ( $I_p$ : 0.1-1.6 MA,  $B_t$ : 0.5-2 T).

confinement characteristics. Additionally, the HL-3 tokamak has exhibited EDA H-mode operation featuring enhanced energy confinement, ELM suppression, sustained through pressure gradient-driven edge quasi-coherent modes. Scenarios aiming for high ion temperature have been developed: e.g. hot-ion L-mode plasmas with strong internal transport barriers (ITBs) reaching core ion temperatures up to  $T_i \sim 5.5$  keV, and H-mode configurations combining ITB and edge transport barrier (ETB) have been achieved with limited NBI power during the last experimental campaign. With the increase in NBI heating power in the ongoing experimental campaign, higher parameters are expected. In parallel, HL-3 has made substantial progress in high  $\beta_N$  plasma development, where stationary  $\beta_N$  values exceeding 3.5 was realized as shown in Fig.1. Various MHD instabilities including fishbone modes, Alfvén eigenmodes (AEs), neoclassical tearing modes (NTMs), and outer region modes have been identified in these discharges. Core NTMs and outer region AEs have been identified as primary  $\beta_N$  limiters: NTMs decelerate  $\beta_N$  growth leading to saturation or disruptions, while outer region AEs can trigger ELM-like events. However, the interaction between micro-tearing mode and energetic-electron-driven geodesic acoustic mode has been found to reduce ambient turbulence, thereby improving energy and particle confinement. The experimental platform has enabled preliminary testing of AI-based NTM prediction algorithms and disruption mitigation systems combining active real-time  $\beta_N$  monitoring with massive gas injection and shattered pellet injection technologies. These developments establish critical infrastructure for managing high-performance plasma operations in future campaigns.

Advanced plasma control strategies for power exhaust have been developed to allow the robust implementation and maintenance of high-performance scenarios. These include using resonant magnetic perturbations for NTM suppression and ELM mitigation, and the synergistic use of ECRH/LHW systems for ELM suppression and heat flux control. Further addressing heat load control concerns in high-performance plasma operation, HL-3 has developed and successfully tested advanced divertor configurations with improved power exhaust capabilities. Comparative analysis of tripod and snowflake configurations as shown in Fig.2 reveals their different heat dissipation properties. The tripod configuration exhibits magnetic flux broadening at the weak-field-side divertor leg, as evidenced by fast camera imaging and configuration superposition diagram in Fig.2(a1). Meanwhile, the snowflake configuration displays heat flow dissipation through its secondary X-point weak magnetic field region as shown in Fig.2(a2), forming a low heat flow region. The time evolution of the ion saturation current measured by divertor Langmuir probes in Fig.2 (b1) and (b2) also demonstrate that the flux reduction at the bottom of the divertor in the snowflake configuration potentially stems from its compressed X-points separation, which creates an expanded weak-field region that reducing heat deposition on the bottom plate and distributing more heat to the strike point. These advanced configurations have been further optimized for heat load control through systematic implementation of RMPs, impurity gas injection, and divertor supersonic molecular beam injection, collectively enhancing heat load control capacity for high-power plasma operations.

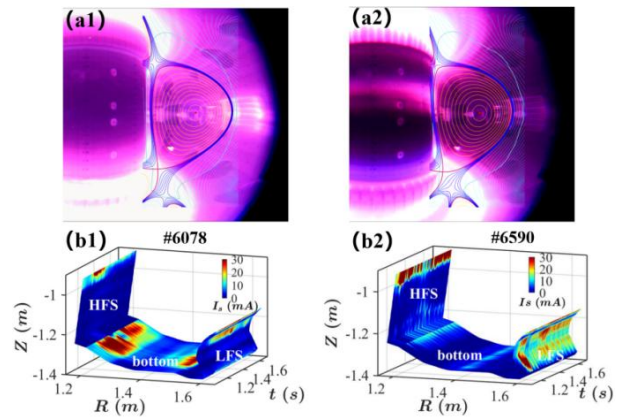


Fig.2 Comparative analysis of tripod and snowflake configurations. Fast camera image and configuration of the (a1) tripod and (a2) snowflake case, ion saturation current profiles by divertor Langmuir probes for the (b1) tripod and (b2) snowflake case.

## ACKNOWLEDGEMENTS

The author (W.L. Zhong) would like to acknowledge all those who have contributed to the HL-3 project. Views and opinions expressed are however those of the author(s) only and do not necessarily reflect those of any entities affiliated with the authors.

## REFERENCES

- [1] Duan X.R. et al Recent advance progress of HL-3 experiments, *Nucl. Fusion* 64 (2024) 11202.
- [2] <https://www.iter.org/node/20687/iter-and-chinas-swip-partner-future>